Psychologic Stress Drives Progression of Malignant Tumors via DRD2/HIF1α Signaling

Huijuan Liu[1,2,3], Jiahuan Yang[1], Yang Zhang[4], Jingxia Han[1], Yuyan Yang[1], Zihan Zhao[1], Xintong Dai[1], Hongqi Wang[1], Xiujuan Ding[1], Yanrong Liu[5], Weilong Zhong[6], Wenqing Gao[2], and Tao Sun[1]

ABSTRACT

Although it is established that the sustained psychologic stress conditions under which patients with tumors often reside accelerates malignant progression of tumors, the molecular mechanism behind this association is unclear. In this work, the effect of psychologic stress on tumor progression was verified using a stress-stimulated tumor-bearing mouse model (Str-tumor). Both D2 dopamine receptor (DRD2) and hypoxia-inducible factor-1α (HIF1α) were highly expressed in the nucleus of Str-tumors. Treatment with trifluoperazine (TFP), a DRD2 inhibitor, elicited better antitumor effects in Str-tumors than the control group. These results indicate that DRD2 may mediate stress-induced malignant tumor progression. DRD2 interacted with von Hippel-Lindau (VHL) in the nucleus, and competitive binding of DRD2 and HIF1α to VHL resulted in reduced ubiquitination-mediated degradation of HIF1α, enhancing the epithelial-mesenchymal transition of tumor cells. TFP acted as an interface inhibitor between DRD2 and VHL to promote the degradation of HIF1α. In conclusion, DRD2 may promote the progression of malignant tumors induced by psychologic stress via activation of the oxygen-independent HIF1α pathway, and TFP may serve as a therapeutic strategy for stress management in patients with cancer.

Significance: This work identifies DRD2 regulation of HIF1α as a mechanism underlying the progression of malignant tumors stimulated by psychologic stress and suggests that DRD2 inhibition can mitigate these stress conditions in patients.

See related commentary by Bernabé, p. 5144

Introduction

Psychologic factors, such as stress, depression, anxiety, and social isolation, have a strong connection with cancer progression (1), which is verified in tumor-bearing mice model (2). Anxiety induced by stress in patients with tumors will decrease their survival time. The molecular mechanism underlying stress-induced malignant progression of tumors has not been elucidated. In addition to the known adrenaline pathway, whether a pathway directly acts on tumor cells is unclear (3). Hypoxia is a feature of the microenvironment in solid tumors (4, 5). Hypoxia promotes the malignant progression and therapeutic resistance of tumors. Hypoxia-inducible factor-1α (HIF1α), whose discovery won a Nobel Prize, mediates the hypoxic response by acting as a transcription factor and affects the proliferation, metastasis, invasion, and epithelial-mesenchymal transformation (EMT) of tumor cells (6). Von Hippel–Lindau (VHL) acts as a subunit of E3 ubiquitin ligase, which targets the alpha subunits of HIF1α for cullin-2 (Cul2)–mediated ubiquitination. The degradation of HIF1α requires nuclear-cytoplasmic trafficking of VHL (7), which occurs under hypoxic conditions. However, the upregulation of HIF1α that is independent of hypoxia is still unclear. Previous studies showed that the expression of HIF1α in tumor tissue increased under chronic stress (8–11), and β2-AR-HIF1α axis can regulate the stress-induced pancreatic tumor growth and angiogenesis (11). The relationship between psychologic stress stimulation and hypoxia-independent HIF1α pathway activation in tumors needs to be further clarified.

D2 dopamine receptor (DRD2) is highly expressed in a variety of cancers and may promote the malignant progression of tumors, such as pancreatic cancer (12, 13) and melanoma (14). Many studies implicated the important role of DRD2 in the pathogenesis of anxiety and depression (15). Stress can induce the pathologic increase of dopamine, which plays a regulatory role mainly by acting on DRD2. Trifluoperazine (TFP), which also has an antitumor effect, is a classical antagonist of DRD2 commonly used in clinics for the treatment of anxiety and depression. Whether the antitumor effect of TFP is related to DRD2 is unclear. Anxiety or depression is a common stress state in cancer patients (16, 17), and the role of DRD2 in stress-induced malignant progression of tumors has not been reported.

In this study, we first evaluated the effect of psychologic stress on tumors using B16F10 and 4T-1 tumor-bearing mice, which had normal immune and gut microbiota systems, stimulated by water immersion and isolation stress. The results showed that psychologic stress can promote tumor growth, and the expressions of DRD2 and HIF1α were up-regulated in tumor cells of the stress stimulation group. TFP exhibited a desirable therapeutic effect on tumors under stress stimulation. Further studies showed that under stress conditions, DRD2 can interact with VHL in the nucleus and inhibit the degradation of HIF1α by ubiquitin-mediated degradation pathway, which promotes the proliferation, migration, and invasiveness of malignant tumors.

[1]State Key Laboratory of Medicinal Chemical Biology and College of Pharmacy, Nankai University, Tianjin, China. [2]Tianjin Key Laboratory of Extracorporeal Life Support for Critical Diseases, Tianjin Third Central Hospital, Tianjin, China. [3]Tianjin Key Laboratory of Early Druggability Evaluation of Innovative Drugs and Tianjin Key Laboratory of Molecular Drug Research, Tianjin International Joint Academy of Biomedicine, Tianjin, China. [4]Department of Anesthesiology, Tianjin Fourth Central Hospital, Tianjin, China. [5]Department of Pathology, Affiliated Hospital of Jining Medical University, Jining Medical University, Jining, Shandong, China. [6]Department of Gastroenterology and Hepatology, Tianjin Medical University General Hospital, Tianjin, China.

H. Liu, J. Yang, Y. Zhang, and J. Han contributed equally to this article.

Corresponding Authors: Tao Sun, Nankai University, State Key Laboratory of Medicinal Chemical Biology, No. 38 Tongyan Road, Haihe River Education Park, Jinnan District, Tianjin, 300450 China. Phone: 13512922691; E-mail: tao.sun@nankai.edu.cn; and Wenqing Gao, Phone: 18512215515; E-mail: gaowenqing0906@126.com

Cancer Res 2021;81:5353–65

doi: 10.1158/0008-5472.CAN-21-1043

Materials and Methods

Materials

The sources of antibodies against the following proteins were obtained: GAPDH (Abcam, Ab181602, RRID:AB_2630358, 1:5000 for Western blot), tubulin (Affinity, AF7010, RRID:AB_2839418, 1:5000 for Western blot); E-cadherin (Affinity, AF0131, RRID: AB_2833315, 1:200 for IF, 1:100 for IHC, and 1:1,000 for Western blot); vimentin [Affinity, BF0071, RRID:AB_2833686, 1:200 for immunofluorescence (IF) and 1:1000 for WB], DRD2 (Abcam, ab30743, RRID:AB_1139814, 1:200 for IF, 1:1000 for Western blot); VHL (Santa Cruz, sc-135657, RRID:AB_2215955, 1:1,000 for Western blot, and 1:100 for IF), HIF1α (Affinity, BF8002, RRID:AB_2846221, 1:1,000 for Western blot, and 1:100 for IHC), ubiquitin (Abcam, ab134953, RRID:AB_2801561, 1:1,000 for immunoprecipitation); flag (Affinity, T0003, RRID:AB_2839412, 1:1000 for Western blot); histone H3 (Affinity, AF0863, RRID:AB_2810277, 1:1,000 for Western blot).

Cell culture and plasmid transfection

B16-F10 cells (RRID:CVCL_0159) and 4T-1 cells (RRID:CVCL_0125) were purchased from KeyGen Biotech and authenticated by short tandem repeat (STR) genotyping. The cells were tested for mycoplasma before use. The cells were cultured in RPMI-1640 medium (HyClone) supplemented with 10% volume for volume (v/v) FBS (Thermo Fisher Scientific) at 37°C and 5% CO_2. The number of passages between cells thawing and use in all the experiments was limited in 15 passages. The human DRD2 gene open reading frame cDNA clone-expression plasmid, N-Flag tag, was purchased from Sino Biological. All the plasmids were transiently transfected into cells using Lipofectamine 2000 (Invitrogen). DRD2 was transiently transfected into B16-F10 cells. Then, the stably transfected cells were screened with hygromycin B for 15 to 30 days. Afterward, the expression of DRD2 was tested by Westen blotting.

Cell-invasion assays

Cell-invasion assay was performed using a 24-well transwell chamber. B16-F10 cells were transfected with DRD2 or SiDRD2. Then, the cells were cultured in a Matrigel-coated top chamber containing serum-free medium. Then, the B16-F10 cells were cultured with or without TFP. The bottom chamber was added with culture medium containing FBS. After 48 hours, cells on the transwell chambers were fixed and then stained with 0.1% crystal violet. The cells that invaded the bottom surface of the chambers were counted in at least five random fields (magnification, ×200; Nikon). Each experiment was performed in triplicate.

Wound-healing and tube formation assay

B16-F10 cells were transfected with DRD2 or SiDRD2 and cultured in 24-well plates. After 24 hours, a scratch was made on the center of the well once the confluence reached about 95%. Then, portions of the cells were treated with TFP, and others remained untreated. The migration rate of cells was assessed by measuring the distance of the scratch. Wound images were photographed every 24 hours using a light microscope (Nikon). Each experiment was performed in triplicate. B16-F10 cells were cultured in a 48-well plate coated with matrigel. Then, the plate was placed in a 37°C incubator, and images were photographed every 12 hours using a light microscope (Nikon).

IF assay

Cells were cultured on glass coverslips (BD) and then fixed with 4% paraformaldehyde (PFA). Samples were then blocked in 5% serum containing 0.1% Triton X-100. Afterward, the cells were incubated with primary antibodies against E-cadherin, vimentin, or DRD2 and secondary antibodies coupled to Alexa Fluor 488 or 594 (Invitrogen). DiD cell membrane red fluorescent dye was used to label the cell membranes. Finally, the cells were stained with DAPI to locate the nucleus. Images were captured with a confocal microscope (Nikon).

Ubiquitination assay

A total of 50 μL 50% protein A/G agarose beads (Pierce) suspended in PBS was incubated with HIF1α antibody (1–2 μg) for 8 hours at 4°C with constant rotation. B16-F10 cells treated with MG132 and with or without DRD2 transfection were lysed by 0.3% Nonidet P-40 lysis buffer (in PBS). Then, anti–HIF1α antibody-conjugated protein A/G beads were incubated with B16-F10 cellular extracts for 12 hours at 4°C. Then, protein A/G beads were boiled in SDS loading buffer and subjected to SDS-PAGE. A polyvinylidene difluoride (PVDF) membrane was incubated with the antiubiquitin antibody and horseradish peroxidase (HRP)–labeled secondary antibodies (Affinity, 1:5000). Finally, target proteins were visualized using enhanced chemiluminescence (ECL) substrate reagents.

Nuclear extract and Western blot

Nuclear extracts from B16-F10 cells with or without treatment were harvested and lysed with nuclear protein lysate buffer (Nuclear and Cytoplasmic Protein Extraction Kit, Sigma). Buffers A and B were used to separate the cytoplasm and nuclear protein, respectively. The protein concentrations were detected, and the proteins were boiled in SDS loading buffer. Proteins from B16-F10 cells were separated by 12% SDS-PAGE and transferred onto PVDF membranes. Then, the membranes were blocked with 5% skimmed milk and incubated with primary antibodies, followed by secondary antibodies. The proteins on PVDF membranes were studied by ECL methods. The autoradiograms were analyzed with Image J software (RRID:SCR_003070) to quantify the band densities.

The tumor-bearing mice experiment

All animal care and experimental procedures complied with the NIH Guide for Care and Use of Laboratory Animals and with the European Communities Council Directive of November 24, 1986 (86/609/EEC). All animal procedures were approved based on the guidelines of the Animal Ethics Committee of Tianjin International Joint Academy of Biotechnology and Medicine [Institutional Animal Care and Use Committee Issue No. TJAB-2017–0225]. C57BL/6J mice (4–6 weeks old, female) were purchased and the mice were allowed to adapt to conditions for 1 week. Before the establishment of stress model, 6 mice were fed in each cage. All the mice were allowed to freely access food and water. Then the mice were divided into stress stimulation group (Str-group) and nonstress stimulation group (non-Str group). The mice in Str-group were treated with water immersion stress (12 hours/day; refs. 18, 19) and housed in isolation for 7 days. The water-immersion stress was performed from 22:00 to 10:00 of the next day, and the floor of the cage was flooded with fresh sterile water at 25 ± 2°C to a depth equivalent to ankle height of the mice. Because the mice are nocturnal, this period of time can avoid disruptions in the sleep cycle of the mice.

And then all the mice in Str-group and non-Str group were inoculated with 1×10^6 B16-F10 cells. After inoculation with tumor cells, the mice in the Str-group were still kept in isolation, but were not subjected to water stress stimulation, which can prevent the tumor rupture or infection after inoculation. One week after the tumor cells were inoculated, the mice in Str-group and non-Str group were

randomly divided into control group, TFP-L group (4 mg/kg/day, intraperitoneally), and TFP-H group (6 mg/kg/day, intraperitoneally), separately. Tumor volume was calculated using the formula: (length × width^2)/2. The weight of each mouse and its food intake were measured every day. After 2 weeks, all the mice were euthanized. And the tumor tissues were collected and fixed with PFA. Then the tissues were embedded in paraffin and cut into 4 μmol–thick sections.

IHC analysis

After dewaxing and hydration, the pathologic sections were treated with 3% hydrogen peroxide for 15 minutes to block the endogenous peroxidase activity. Citrate buffered saline was used for antigen retrieval for 15 minutes at 95°C. Then, the sections were blocked for 20 minutes with normal goat serum (NGS) at room temperature. Next, the sections were incubated with primary antibodies overnight at 4°C. Afterward, the sections were incubated with the HRP goat-antirabbit secondary antibody for 30 minutes. Finally, the slides were stained with diaminobenzidine (DAB) and hematoxylin. Then the slides were observed under a microscope and photographed.

Dual-luciferase reporter gene assay

B16-F10 cells were seeded in 96-well plates. After 24 hours, the luciferase reporter plasmids of *snail1, snail2, twist1*, and *twist2* were transfected separately into the cells and treated with TFP. After 48 hours, luciferase activities were measured by using Dual-Luciferase Reporter Assay kit. The experiment was performed in triplicate.

In situ proximal ligation assay analysis of B16-F10 cells

Glass slides with ethanol-fixed cells were blocked in 20% goat serum (Invitrogen), and the cells were incubated with antibodies of DRD2 and VHL. Then, the slides were added with Duolink Proximal Ligation Assay (PLA) probe (Sigma) and ligation solution. The coupled reaction of interaction proteins was amplified using the amplification solution. Afterward, the nuclear of cells was stained with DAPI. Finally, the fluorescent spot signal (represent the interaction between DRD2 and VHL) was observed with a confocal microscope (Nikon).

Data analysis

The data were expressed as means ± SD. The statistical significance of differences among multiple groups was determined with analysis of variance and unpaired Student *t* test using GraphPad Prism (RRID: SCR_002798). Statistical significance was considered at $P < 0.05$.

Results

TFP suppressed the progression of malignant tumors under psychologic stress condition

B16F10 and 4T-1 tumor-bearing mice under stress stimulation were used to evaluate the effect of psychologic stress on tumors, which was induced by water immersion and social isolation (**Fig. 1A**). The water immersion stress model can simulate the state of an individual in unavoidable psychologic stress. Isolation feeding stress can simulate the stress state caused by social isolation. TFP, a psychiatric intervention drug commonly used in clinical settings, was used for the trial treatment. B16-F10- or 4T-1–bearing C57BL/6J mice were stimulated by water immersion for 12 hours/day and fed in isolation. Then, the mice were treated with low- (TFP-L, 4 mg/kg/day, intraperitoneally) or high-dose (TFP-H, 6 mg/kg/day, intraperitoneally) of TFP. The experimental results showed that the tumor growth of mice under stress condition (Str-tumor) was faster than that of the control group without stress stimulation (**Fig. 1B**). Tumor weight in the Str-group was about 1.5 times that of the control group. Evidently, the tumor volume (**Fig. 1B**) and weight (**Fig. 1C**) were inhibited by TFP. **Figure 1D** and **E** show the representative tumor images. The DRD2 inhibitor TFP showed a better antitumor effect on tumor-bearing mice exposed to psychosocial stress than the unexposed ones. In the control group, the tumor inhibition rates (B16F10 model) of the TFP-L and TFP-H groups were 13% and 32%. Under the stress-stimulated condition, the tumor inhibition rate (B16F10 model) in the TFP-L and TFP-H groups reached 46% and 57%, respectively. The same trend was observed in the 4T-1 tumor-bearing model. These results suggest that DRD2 may mediate the effect of stress stimulation–induced malignant progression of tumors.

DRD2 translocated into the nucleus in tumor tissues of mice under stress stimulation

Based on the above hypothesis, DRD2 expression level was detected in tumor tissues of each group. The results showed that the expression level of DRD2 in B16F10 (**Fig. 1F** and **G**) and 4T-1 (**Fig. 1H** and **I**) tumor tissues under stress condition was higher than those of without stimulation. We observed that the expression of DRD2 in nucleus was strongly positive, and the expression ratio of nucleus to cytoplasm was upregulated in tumor tissues under stress condition. Western blot results also showed that the expression level of DRD2 in the nuclei of stress-stimulated tumor tissues was higher than that without stimulation (**Fig. 1J**). The mRNA-sequencing (mRNA-seq) data of melanoma cancer samples in The Cancer Genome Atlas database (TCGA; https://portal.gdc.cancer.gov/) were obtained to study the main functions and signaling pathways that may be affected by DRD2. Gene Ontology (GO) and Kyoto Encyclopedia of Genes and Genomes (KEGG) enrichment analysis were used to analyze the differential genes affected by DRD2. The results showed that DRD2 mainly affected the pathways of ubiquitin proteasome, HIF1 signal, and Janus kinase/signal transducers and activators of transcription (**Fig. 1K**). The mRNA-seq data of tumor tissues were also obtained to study the main functions affected by stress stimulation. The results showed that the proteins affected by stress stimulation were mainly enriched in the HIF1 signal pathway (**Fig. 1L**).

DRD2 promoted migration, invasion, clonogenicity, and tube formation of tumor cells

Overexpression and RNAi of DRD2 in B16-F10 cells were used to evaluate the effect of DRD2 on tumor cells. Scratch experiment showed that overexpression of DRD2 can promote the migration of B16-F10 cells (**Fig. 2A** and **B**), and DRD2 silencing markedly inhibited the migration of B16-F10 cells. Tube formation assay indicated that DRD2 enhanced the tube formation ability of B16-F10 and A375 cells (**Fig. 2C** and **D**). Transwell experiment results showed that DRD2 overexpression enhanced the invasion ability of melanoma cells (**Fig. 2E** and **F**), whereas DRD2 silencing decreased the number of invasion cells. Clone formation assays showed that DRD2 promoted the clonogenicity of B16-F10 cells (**Fig. 2G** and **H**). Proliferation assay showed that DRD2 can promote the cell viability of B16-F10 and A375 cells (**Fig. 2I**). We also observed that the overexpression of DRD2 led to decreased E-cadherin expression (epithelial marker of EMT) and increased vimentin expression (mesenchymal marker of EMT), as detected by Western blot (**Fig. 2J**) and IF (**Fig. 2K** and **L**). These findings indicate that DRD2 overexpression can promote the EMT of tumor cells.

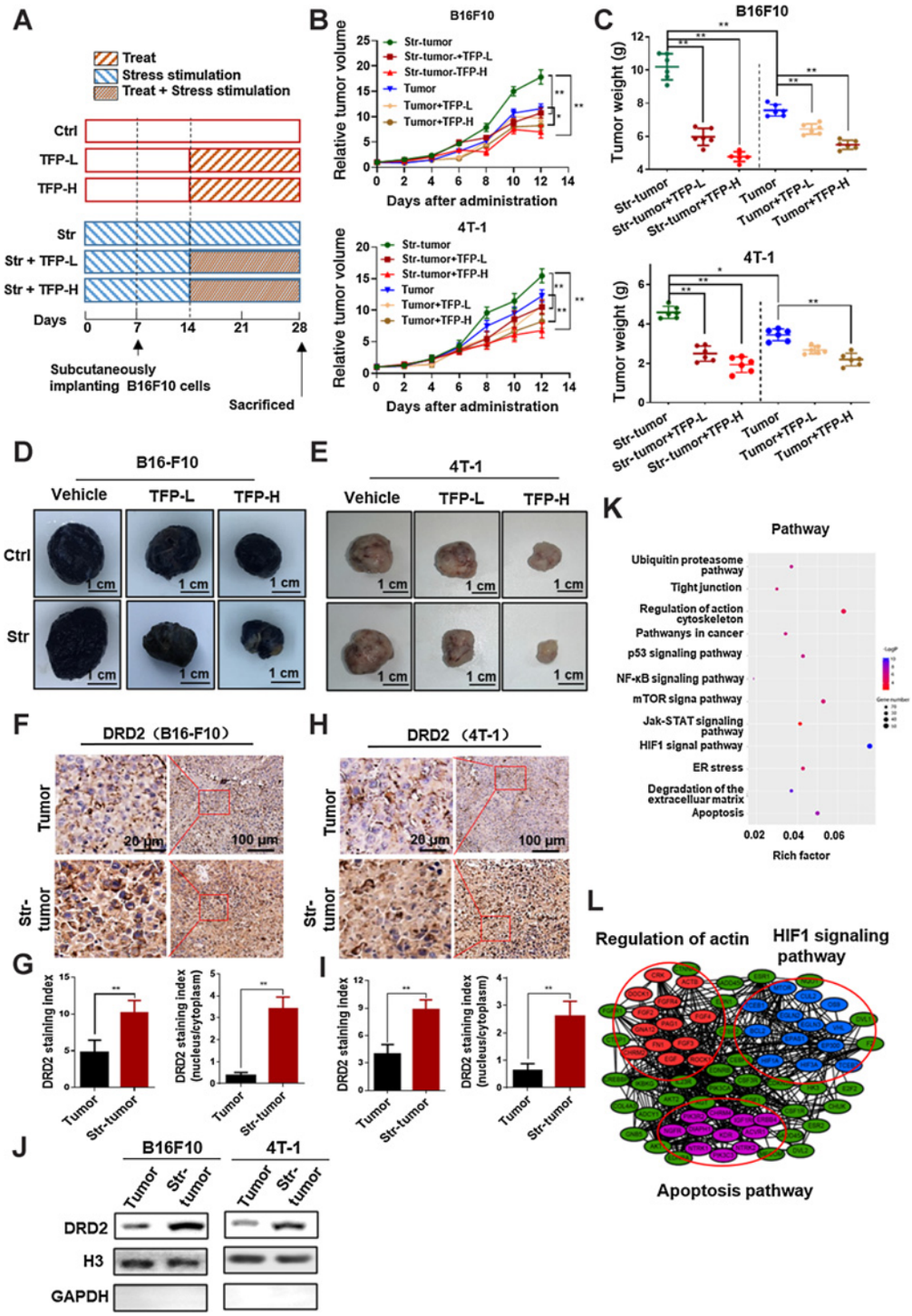

Figure 1.

DRD2 may promote the malignant progression of melanoma and breast cancer under psychologic stress condition. **A,** Construction scheme of Str-tumor. **B** and **C,** Changes in the volume and weight of tumors treated with TFP in stress stimulation B16F10 and 4T-1 tumor-bearing mice. **D** and **E,** Representative images of tumors in each group. **F** and **G,** IHC analysis of DRD2 expression levels in B16F10 melanoma tissues with or without stress stimulation. Scores of staining intensity and the nucleus/cytoplasm expression ratio of DRD2 were also analyzed. **H** and **I,** IHC analysis of DRD2 expression levels in 4T1 breast cancer tissues with or without stress stimulation. **J,** Western blot analysis of DRD2 expression levels in the nuclei of B16F10 and 4T1 tumor tissues with or without stress stimulation. **K,** KEGG enrichment analysis of the differential expression genes affected by DRD2. **L,** Protein–protein interaction analysis of differentially expressed proteins in tumor tissues affected by stress stimulation. *, $P < 0.05$; **, $P < 0.01$.

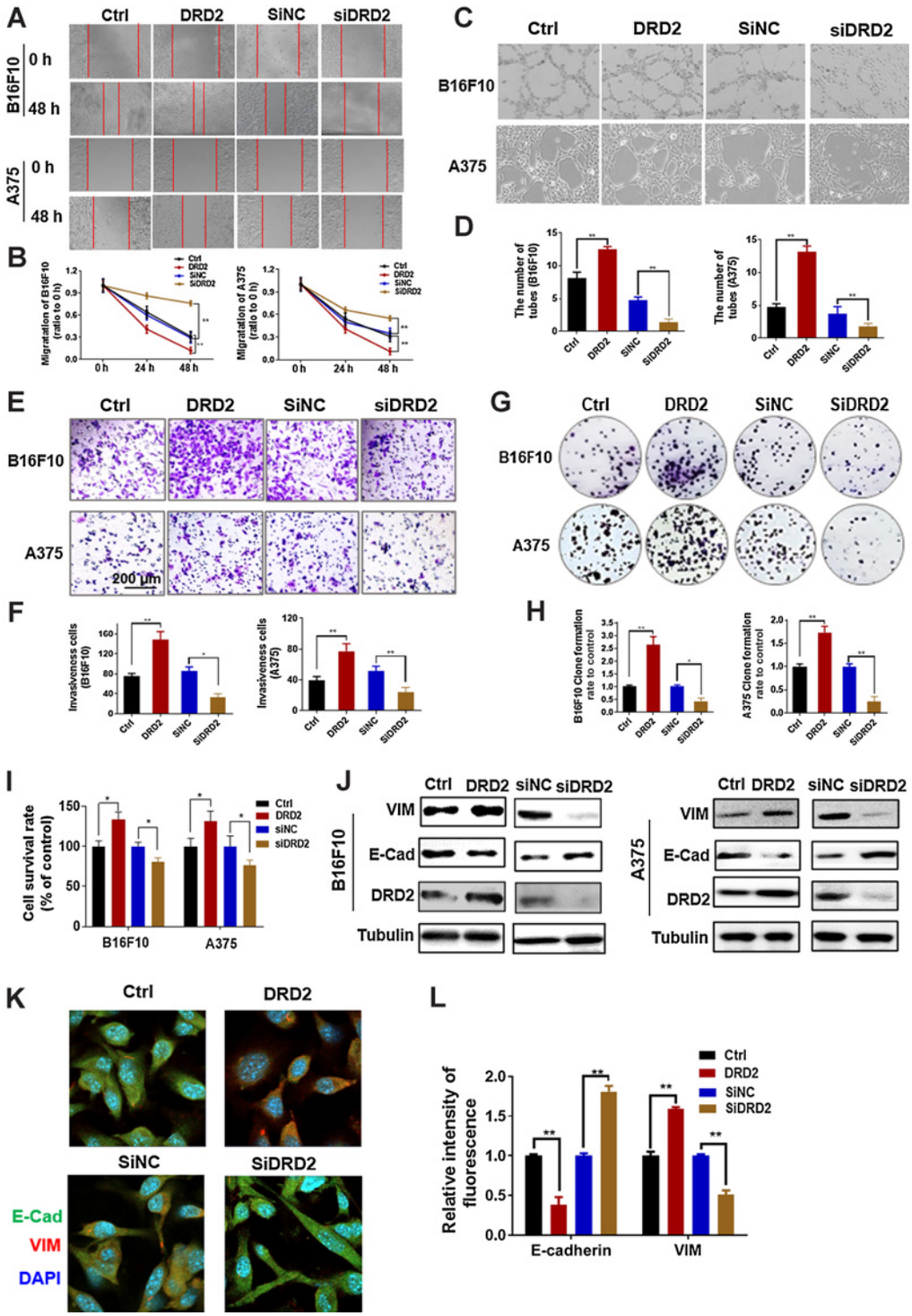

Figure 2.

DRD2 overexpression promotes the metastasis, invasion, tube formation, and cloning formation of tumor cells. **A** and **B,** Wound-healing assay of B16-F10 and A375 cells treated with DRD2 overexpression vectors or siRNA. **C** and **D,** Effect of DRD2 on vasculogenic mimicry formation of B16-F10 and A375 cells detected by tube formation assay. **E** and **F,** Effect of DRD2 on the invasion ability of B16-F10 and A375 cells. **G** and **H,** Effect of DRD2 on cloning formation ability of B16-F10 and A375 cells. **I,** Effect of DRD2 on the cell viability of B16F10 and A375 cells. **J,** Effect of DRD2 on the expression E-cadherin and vimentin detected by Western blot. **K** and **L,** Effect of DRD2 on the expression of E-cadherin and vimentin detected by IF. Each experiment was performed in triplicate. Results are shown as means ± SD, *, $P < 0.05$; **, $P < 0.01$.

Dopamine promoted the nuclear localization of DRD2

DRD2 translocation into the nucleus has not been reported in previous studies. Thus, we further explored the induction factors of DRD2 nuclear translocation. IF results showed that DRD2 expression (**Fig. 3A** and **B**) and nucleus location (**Fig. 3C**) were upregulated when melanoma cells were treated with dopamine or DRD2 overexpression. The hypoxic environment can also induce the overexpression of DRD2. However, hypoxia cannot effectively promote the nucleus localization of DRD2 compared with dopamine. Western blot results also showed that DRD2 and HIF1α expressions in nucleus were up-regulated when B16-F10 cells and A375 cells were treated with dopamine and DRD2 overexpression (**Fig. 3D**). We also detected the relationship between dopamine-induced DRD2 nucleus localization and HIF1α expression under nonhypoxia condition. Western blot results revealed that DRD2 expression dose-dependently increased in the nucleus of B16-F10 cells treated with different dopamine concentrations (**Fig. 3E**). The effect of DRD2 on the expression of HIF1α was also detected in DRD2-knockdown B16-F10 and A375 cells. The results showed that the expression of HIF1α decreased in DRD2-knockdown B16-F10 and A375 cells (**Fig. 3F** and **G**). HIF1α expression level was also detected in tumor tissues under stress condition. The results revealed that the expression level of HIF1α in B16F10 tumor tissues under stress condition was higher than that without stress stimulation. The expression of HIF1α in the nucleus was strongly positive, and the expression ratio of nucleus to cytoplasm was upregulated in tumor tissues under stress condition (**Fig. 3H–J**).

DRD2 physically interacted with VHL under dopamine-stimulation condition

A prediction software (FpClass website: http://dcv.uhnres.utoronto.ca/FPCLASS/; ref. 20) was used to predict the interaction between DRD2 and HIF1α. The predicted results showed no direct physical interaction between DRD2 and HIF1α. However, some proteins can interact with both DRD2 and HIF1α (**Fig. 4A**). VHL is an E3 ubiquitin ligase that targets HIF1α for proteasomal degradation, which is closely related to the degradation of HIF1α. So we further verified the interaction between DRD2 and VHL. The interaction between DRD2 and VHL was verified by molecular docking (Score: -5.052), which indicated that DRD2 may interact with VHL (**Fig. 4B**). Based on the above results, we further conducted the biochemical experiment to research the relationship between DRD2 and HIF1α in tumor cells. Coimmunoprecipitation (co-IP) results showed no interaction between DRD2 and HIF1α (**Fig. 4C**). Western blot results showed that DRD2 overexpression can increase the content of HIF1α in melanoma cells, whereas VHL overexpression decreased the HIF1α expression (**Fig. 4D**). PLA and co-IP experiments were performed to verify the interaction between DRD2 and VHL. PLA results showed that the red dots caused by DRD2 and VHL interaction increased in the nucleus of melanoma cells stimulated by dopamine or hypoxia (**Fig. 4E** and **F**). DRD2 coimmunoprecipitated with VHL in the nucleus of melanoma cells treated with dopamine (**Fig. 4G**). VHL can directly bind with elongin C (EloC), which can bind EloB, Cul2, and RING box protein-1 to form a multimeric complex. The VHL complex can target HIF1α for ubiquitin-mediated degradation. The effect of DRD2 on the interaction of HIF1α/VHL and VHL/EloC was studied. Co-IP results showed that DRD2 overexpression can interfere with the interaction of HIF1α/VHL (**Fig. 4H**) and VHL/EloC.

DRD2 overexpression inhibited the ubiquitin-mediated degradation of HIF1α

Based on the above results, we assumed that the interaction between DRD2 and VHL can competitively inhibit the interaction between HIF1α and VHL and ubiquitination degradation of HIF1α. We further verified this hypothesis. Cycloheximide chase assays were designed to detect the half-life of HIF1α influenced by DRD2. The results indicated that DRD2 overexpression prolonged the half-life of HIF1α (**Fig. 4I** and **J**). Meanwhile, HIF1α half-life decreased in DRD2-deficient cells (**Fig. 4K** and **L**). Melanoma cells were also treated with proteasome inhibitor MG132. The reduced protein level of HIF1α due to DRD2 knockdown can be rescued by proteasome inhibitor MG132 (**Fig. 4M**). These results revealed that DRD2 mainly regulates the stability of HIF1α. The ubiquitination assays confirmed that the ubiquitinylate level of HIF1α was reduced in DRD2-overexpressing cells with MG132 treatment (**Fig. 4N**). These results indicate that DRD2 can stabilize HIF1α by inhibiting HIF1α degradation through the proteasome pathway.

TFP targeted the interaction interface of DRD2 and VHL and inhibited the expression of HIF1α

Molecular docking results revealed that TFP can bind to the interface between DRD2 and VHL (**Fig. 5A**). This result reveals the possible antitumor mechanism of TFP. The co-IP results showed that TFP can inhibit the interaction between DRD2 and VHL (**Fig. 5B**). PLA results showed that the red dots caused by DRD2 and VHL interaction decreased in the nucleus of melanoma cells in TFP treated groups (**Fig. 5C**). Western blot experiment also unveiled that TFP decreased the expression of HIF1α in B16-F10 cells under hypoxia or dopamine stimulation (**Fig. 5D**). Wound-healing assay revealed that dopamine promoted the migration of tumor cells, and the cells treated with TFP inhibited the migration of B16-F10 and A375 cells (**Fig. 5E** and **F**) induced by dopamine. Tube formation, transwell, and clone formation assays exhibited that TFP decreased the tube formation (**Fig. 5G** and **H**), invasion ability (**Fig. 5I** and **J**), and clone formation ability (**Fig. 5K** and **L**) of tumor cells induced by dopamine.

TFP inhibited the EMT of tumor cells under nonhypoxia condition

HIF1α is closely related to tumor invasion and metastasis and EMT in hypoxia. We evaluated the effect of TFP on EMT in nonhypoxia condition induced by dopamine/DRD2. qPCR results showed that TFP can inhibit the mRNA expression of Twist1, Gltu1, vascular endothelial growth factor-A (VEGF-A), and TGF-β1 in A375 cells (**Fig. 6A**). Luciferase reporter gene assay showed that TFP inhibited the activation of EMT-related transcription factors (Twist1, Twist2, Sanil1, and Snail2), which can be regulated by HIF1α (**Fig. 6B**). Western blot analysis revealed that TFP treatment upregulated the expression level of E-cadherin and downregulated the expression level of vimentin in tumor cells (**Fig. 6C**). The results were also supported by IHC assay of tumor tissues in the Str-group (**Fig. 6D–F**). The results of IHC experiments confirmed that TFP can inhibit the expression of vimentin, HIF1α, VEGFA, and Twist1 (**Fig. 6D–F**) in tumor tissues of the Str-group. The *in vivo* experiment also showed that TFP exhibited minimal effects on the tumors when DRD2 was knocked down using the shRNA of DRD2 (**Fig. 6G** and **H**), which indicated that TFP plays the antitumor role mainly through targeting DRD2.

Discussion

Chronic behavioral stress leads to high levels of catecholamines (eg. norepinephrine) and promotes the growth of tumors (21, 22). Behavioral stress can also enhance the invasion and metastasis of tumor cells, thus promoting the evolution of malignant tumors (2, 23, 24). Arranz and colleagues confirmed that chronic stress is associated with tumor

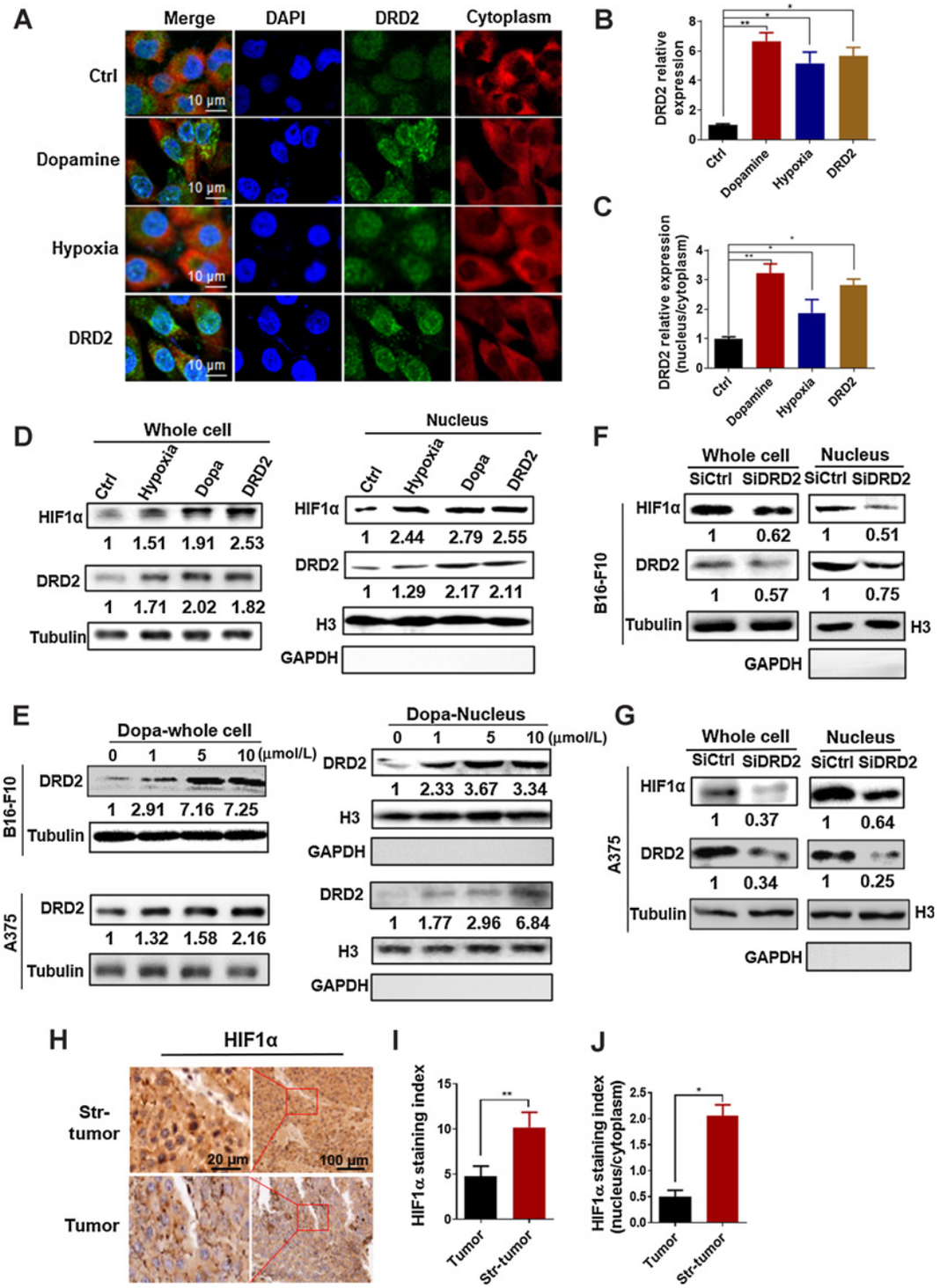

Figure 3.

Dopamine or hypoxia stimulation promotes nuclear localization of DRD2. **A,** Localization and expression of DRD2 detected by IF assays in dopamine, hypoxia, or DRD2 overexpression–treated melanoma cells. **B,** Pearson correlation coefficient of DRD2 and nucleus analyzed by IF assays. **C,** Nucleus-to-cytoplasmic ratio of DRD2 in each group. **D,** DRD2 and HIF1α expressions in nucleus extracts of B16-F10 cells with hypoxia, dopamine, or DRD2-overexpression treatment. **E,** Changes in DRD2 expression level in B16-F10 and A375 cells treated with different concentrations of dopamine. **F** and **G,** Effect of DRD2 on the expression of HIF1α in B16-F10 and A375 cells. **H–J,** IHC analysis of HIF1α expression levels in B16F10 melanoma tissues with or without stress stimulation. Results are shown as means ± SD. *, $P < 0.05$; **, $P < 0.01$.

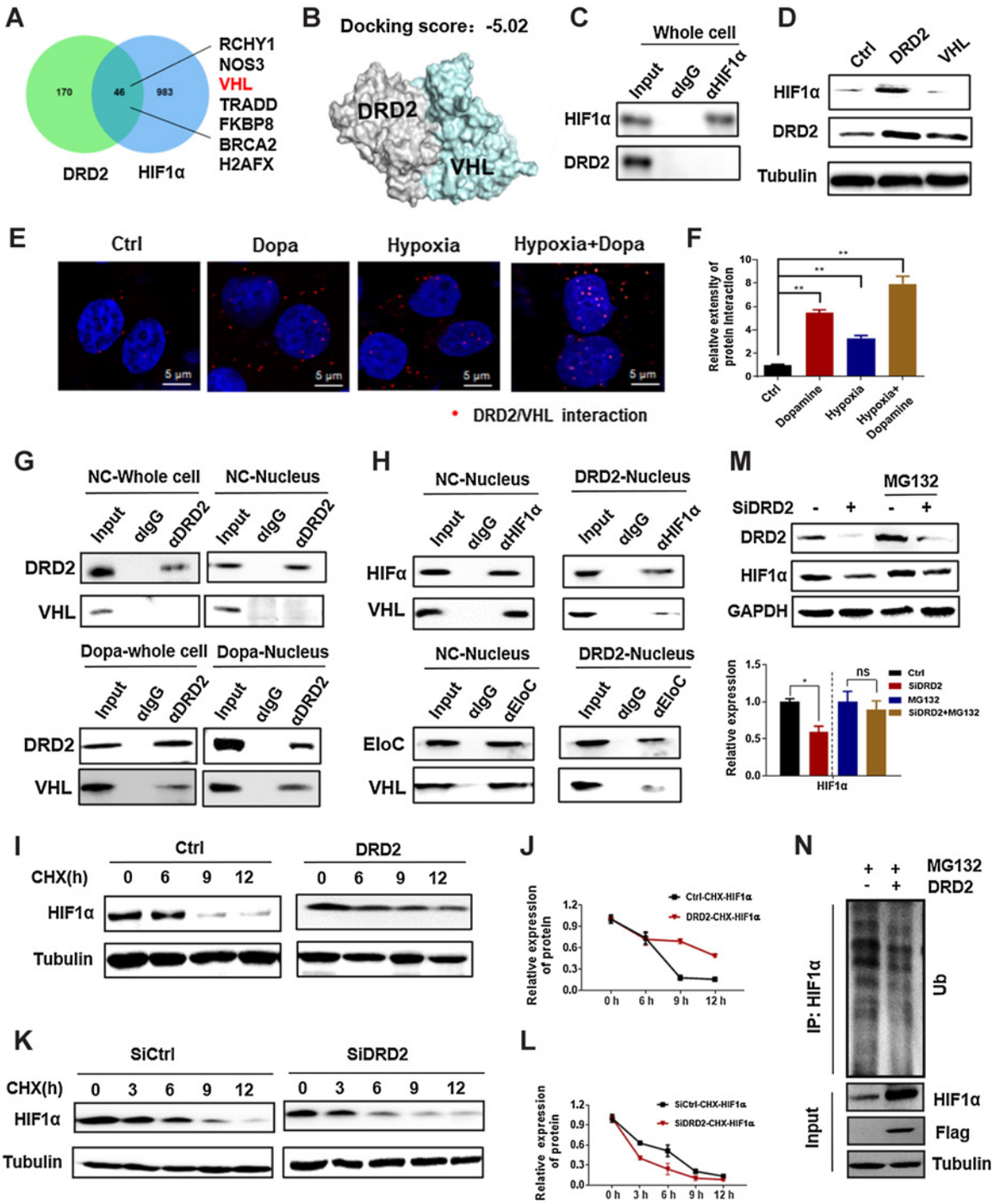

Figure 4.

DRD2 overexpression inhibited the ubiquitin-dependent degradation of HIF1α. **A,** Venn diagram of proteins that interacted with DRD2 and HIF1α, as predicted by FPclass website. **B,** Molecular docking results of DRD2 and VHL. **C,** Co-IP results of DRD2 and HIF1α. **D,** Effect of DRD2 and VHL on the content of HIF1α detected by Western blotting. **E** and **F,** Interaction between DRD2 and VHL validated by Duolink PLA experiments. **G,** Interaction of DRD2 and VHL detected by co-IP assay. Nucleus lysates of melanoma cells treated with or without dopamine were immunoprecipitated with anti-DRD2 antibodies, followed by Western blotting detection. **H,** Interaction of HIF1α/VHL and Eloc/VHL detected by co-IP assay in the nucleus lysates of DRD2-overexpressing melanoma cells. **I–L,** Effect of DRD2 on the degradation of HIF1α. Cells were transfected with DRD2 overexpression vector or siRNA treated with cycloheximide (CHX) and harvested at the indicated time followed by Western blot detection of HIF1α. **M,** Effect of DRD2 on the expression of HIF1α. Melanoma cells treated with DRD2 siRNA and incubated with or without 5 μmol/L MG132. **N,** Effect of DRD2 on the content of ubiquitin binding to HIF1α. DRD2-overexpressing cells treated with MG132, and cellular extracts were prepared for co-IP assay with anti–HIF1α antibody, followed by Western blotting detection of ubiquitin. siRNA, small interfering RNA. ns, nonsignificant; *, $P < 0.05$; **, $P < 0.01$.

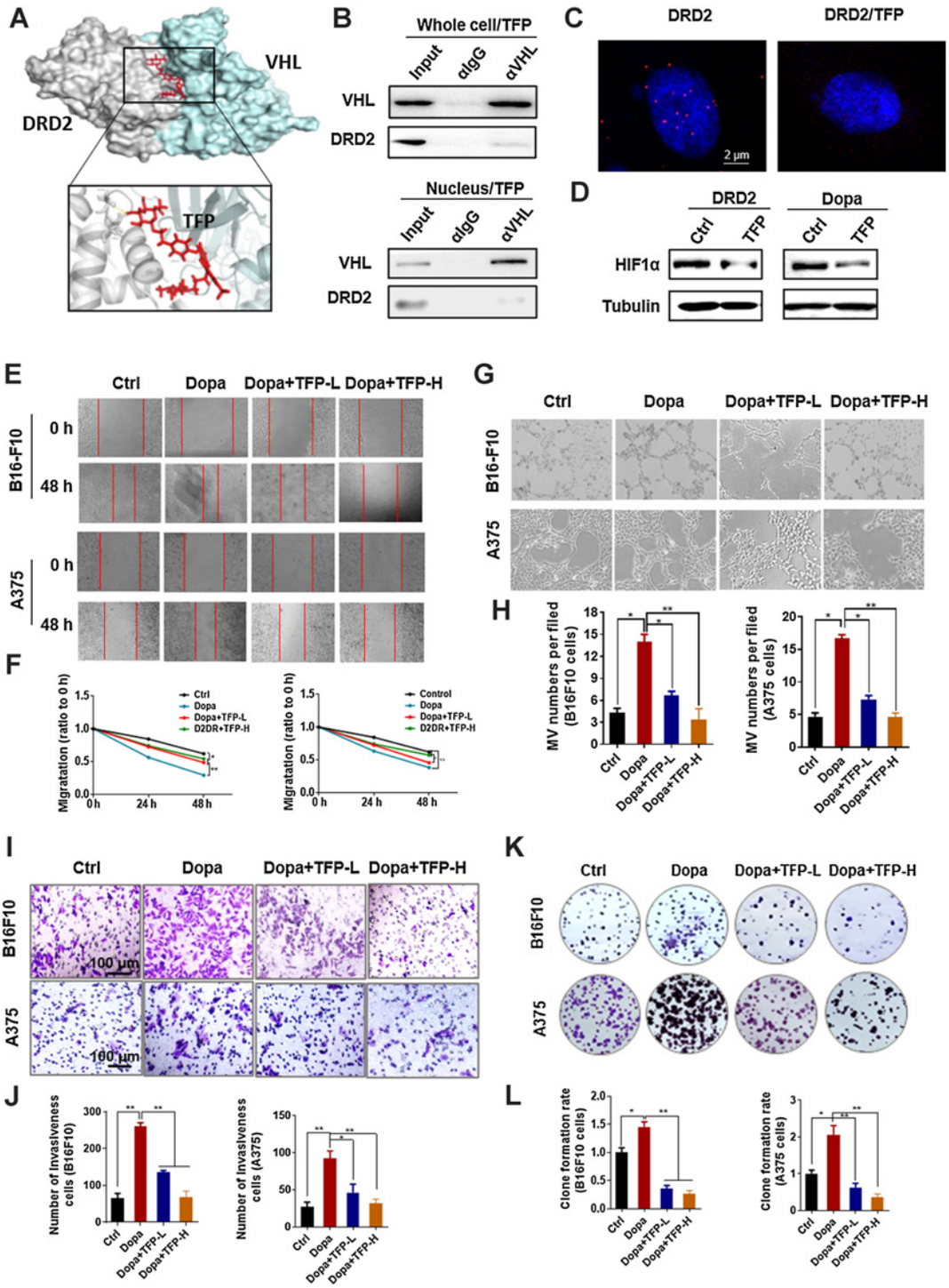

Figure 5.

TFP targeted the interaction interface of DRD2 and VHL and inhibited the metastasis, invasion, tube formation, and cloning formation of melanoma cells. **A,** Molecular docking results showed that TFP can bind to the interface between DRD2 and VHL. **B** and **C,** Effect of TFP on DRD2 and VHL interaction in dopamine-treated melanoma cells detected by co-IP assay and PLA assay. **D,** Effect of TFP on the expression of HIF1α in melanoma cells exposed to DRD2 overexpression or dopamine stimulation. **E** and **F,** Effect of TFP on the migration ability of dopamine-treated B16-F10 and A375 cells. **G** and **H,** Effect of TFP on the tube formation ability of dopamine-treated B16-F10 and A375 cells, respectively. **I** and **J,** Effect of TFP on the invasion ability of dopamine-treated B16-F10 and A375 cells, respectively. **K** and **L,** Effect of TFP on the cloning formation of dopamine-treated B16-F10 and A375 cells, respectively. Each bar represents the mean ± SD for biological triplicate experiments. *, $P < 0.05$; **, $P < 0.01$.

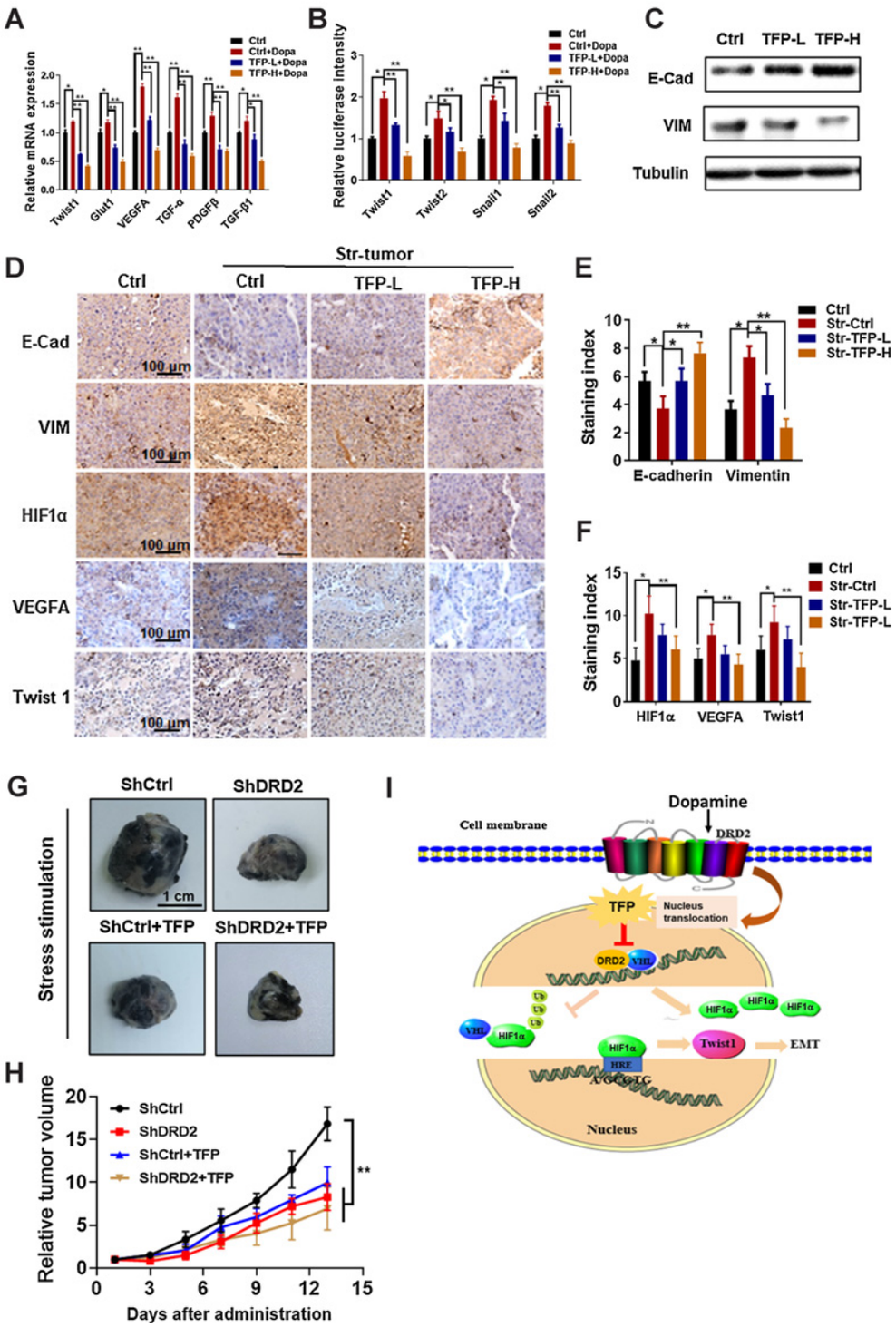

Figure 6.

TFP inhibits EMT of melanoma cells. **A,** Effect of TFP on the mRNA expression of EMT-related genes (Twist1, TGF-β1, and VEGFA) of A375 cells detected by qPCR. **B,** Effect of TFP on the activity of transcription factors related to EMT in A375 cells, as detected by dual-luciferase reporter assay. **C,** Effect of TFP on the EMT markers (E-cadherin and vimentin) in dopamine-treated melanoma cells. **D–F,** IHC analysis of E-cadherin, vimentin, HIF1α, VEGFA, and Twist1 in melanoma tumor tissues of mice under stress stimulation. Representative images and staining scores are shown. Scale bar, 100 μm. **G** and **H,** Effect of TFP on shDRD2/B16F10 xenograft tumors in C57BL/6J mice under stress stimulation ($n = 6$). **I,** Molecular mechanism of TFP inhibiting the progression of malignant tumors induced by psychologic stress. Each bar represents the mean ± SD for biological triplicate experiments. *, $P < 0.05$; **, $P < 0.01$.

growth in a chronic-stress mouse model (25). However, the molecular mechanism of stress in promoting the evolution of malignant tumors is still unclear. Chronic stress–induced epinephrine promotes breast cancer stem-like properties via lactate dehydrogenase A–dependent metabolic rewiring (3). Norepinephrine induced by chronic stress can also promote the phosphorylation of L-type voltage-dependent calcium channels through the β-adrenergic receptor-protein kinase A pathway, thereby promoting lung tumorigenesis (26). In this work, we observed that the growth rate of tumors in the Str-group was higher than that of the control group. As an antipsychotropic drug, DRD2 antagonist TFP has a desirable therapeutic effect on melanoma-bearing mice under pressure stimulation. Thus, DRD2 may mediate the stress-induced tumor-malignant progression. DRD2 is highly expressed in pancreatic, breast, ovarian, and lung cancers and other tumor tissues and can promote the proliferation of these tumor cells. However, DRD2 also has antitumor effects on several tumor cells. DRD2 agonists and inhibitors have been reported to possess antitumor effects. Thus, DRD2 may play different roles in various types of cancer. These previous studies did not consider the background of psychologic stress. Based on the results of the current work, we speculate that psychologic stress station and dopamine stimulation may be the main influencing factors of DRD2 in promoting tumor progression.

The IHC results of tumor tissues showed increased DRD2 and HIF1α expression levels. Nuclear localization of DRD2 was significantly enhanced in the Str-group. DRD2 belongs to the G protein coupled receptor (GPCR) family, which consists of a single polypeptide chain that loops through the cell membrane seven times to form an interhelical cavity of seven alpha-helical transmembrane domains (27). The location of DRD2 in nucleus and its function have been rarely reported in previous research. Traditionally, GPCR is thought to be located on the cell surface, where it transmits extracellular signals to the cytoplasm. Several studies indicated that certain GPCRs are localized to various subcellular compartments such as the nucleus. Intracellular GPCRs can function independently, governing processes, such as synaptic plasticity (28), myocyte contraction (29), and angiogenesis (30). Nuclear localization can drive α1-adrenergic receptor oligomerization and signaling in cardiac myocytes. Coagulation factor II receptor-like 1 (F2rl1) can translocate from the plasma membrane to the cell nucleus after stimulation. In the nucleus, F2rl1 facilitates recruitment of the transcription factor Sp1 to trigger VEGFA expression and neovascularization (30). Our previous work showed that protease-activated receptor-1 can increase the expression of endothelial markers and enhance vasculogenic mimicry formation by upregulating Twist1 through thrombin binding (31). In this study, we discovered that DRD2 showed evident nuclear translocation under stress stimulation, but this phenomenon wasn't evident under normal expression. Dopamine and DRD2 overexpression can also promote the nuclear translocation *in vitro*. Therefore, we speculate that nuclear translocation of DRD2 may be due to the abnormal vesicular traffic of tumor cells rather than the assistance of nuclear entry guidance sequence or chaperone protein.

Hypoxia is a marker of tumor microenvironment, and the expression of HIF1α in solid tumors promotes the proliferation, metastasis, angiogenesis, and drug resistance of tumors (32–34). VHL functions as VBC/Cul-2 particle recognition protein by promoting the recruitment of the alpha subunits of HIF1α for Cul2-mediated ubiquitination. VHL is closely related to the EMT of tumor cells (35). VHL can shuttle between nucleus and cytoplasm, and its nuclear localization plays an important role in its antitumor effect (36). HIF1α can be degraded in the nucleus or cytoplasm. Our study showed that HIF1α can enter the nucleus and function under non hypoxia conditions. HIF1α cannot be degraded by ubiquitination because DRD2 protected HIF1α from being recognized by VHL ubiquitination system. This process is a non–oxygen-dependent HIF1α pathway that may be specific to tumor cells. However, hypoxic conditions will enhance this pathway. Research shows that VHL mediates the ubiquitination of HIF1α in the nuclear compartment prior to its exportation to the cytoplasm (7). In this work, the mechanism of DRD2 entry into the nucleus and its regulatory effect on HIF1a in nonhypoxia condition were evaluated. The interaction of DRD2 and VHL can competitively inhibit the interaction between HIF1α and VHL and block the ubiquitination degradation of HIF1α, thus promoting the proliferation, migration, and invasiveness of tumor cells under stress stimulation condition. The transcription products of HIF1α include Twist1, VEGFA, and TGF-β1. These target genes are closely related to the evolution of malignant tumors. In general, hypoxia can induce HIF1α high expression and promote its transcriptional activity. However, this study revealed that dopamine-induced DRD2 nuclear translocation can inhibit the degradation of HIF1α, thus promoting the expression of downstream genes and progression of malignant tumors.

Phenothiazines are antipsychotic drugs that act as DRD2 antagonists, and they have been widely used to treat anxiety disorders. Evidence indicates that they interfere with various cellular processes and have novel properties, such as antimicrobial, antiprionic (37), and anticancerous activities (38). TFP is a classic phenothiazine antipsychotropic drug that can improve anxiety symptoms in patients with abnormal behavior. In addition, TFP has certain antitumor effect on triple-negative breast cancer (39) and glioblastoma (40), but the underlying molecular mechanism of its antitumor effect is unclear. The diversity of pharmacologic effects of DRD2 inhibitors also indicates the complexity of downstream signaling pathways affected by DRD2. These pathways have not been fully elucidated. In this work, we observed that TFP has an improved therapeutic effect on tumor-bearing mice under pressure stimulation. We explored the molecular mechanism behind this phenomenon. The results showed that TFP can inhibit the interaction of DRD2 and VHL and promote the ubiquitin-dependent degradation of HIF1α. In addition, TFP can inhibit the invasion, metastasis, vasculogenic mimicry formation, and EMT of tumor cells under dopamine stimulation. In this study, the TFP-H group (6 mg/kg) has a good antitumor effect, which is about twice the clinical dose of TFP as a drug for the treatment of anxiety. Clinical studies have shown that TFP can induce extrapyramidal reactions, and long-term application may lead to the tardive dyskinesia. Therefore, the application of TFP as a therapeutic drug for patients with cancer with psychosocial stress background needs further clinical safety and effectiveness evaluation.

In conclusion, this work provides evidence that the interaction between DRD2 and VHL in nucleus may establish a hypoxia-independent HIF1α pathway, which mediates the malignant evolution of tumor-bearing mice under psychosocial stress stimulation. TFP can inhibit the interaction between DRD2 and VHL and promote the degradation of HIF1α, thus exerting an antitumor effect (**Fig. 6I**). TFP may become a potential therapeutic drug for the treatment of patients with tumors with psychosocial stress background.

Authors' Disclosures

No disclosures were reported by the authors.

Authors' Contributions

H. Liu: Methodology, writing–review and editing. **J. Yang:** Data curation, investigation. **Y. Zhang:** Supervision. **J. Han:** Validation, investigation. **Y. Yang:** Validation, methodology. **Z. Zhao:** Methodology. **X. Dai:** Methodology. **H. Wang:** Formal analysis. **X. Ding:** Resources. **Y. Liu:** Supervision. **W. Zhong:** Validation. **W. Gao:** Resources. **T. Sun:** Conceptualization, funding acquisition.

Acknowledgments

This work was supported by National Natural Science Funds of China (grant nos. 82073205, 81872374, 81703581, 81972629, and 81871972), The National Youth Talent Support Program (2020), Tianjin Science Fund for Distinguished Young Scholars (19JCJQJC63200), Hundred Young Academic Leaders Program of Nankai University, and The Taishan Scholars Program of Shandong Province (tsqn201909193).

The costs of publication of this article were defrayed in part by the payment of page charges. This article must therefore be hereby marked *advertisement* in accordance with 18 U.S.C. Section 1734 solely to indicate this fact.

Received April 4, 2021; revised April 16, 2021; accepted July 23, 2021; published first July 28, 2021.

References

1. Moreno-Smith M, Lutgendorf SK, Sood AK. Impact of stress on cancer metastasis. Future Oncol 2010;6:1863–81.
2. Hasegawa H, Saiki I. Psychosocial stress augments tumor development through beta-adrenergic activation in mice. Jpn J Cancer Res 2002;93:729–35.
3. Cui B, Luo Y, Tian P, Peng F, Lu J, Yang Y, et al. Stress-induced epinephrine enhances lactate dehydrogenase A and promotes breast cancer stem-like cells. J Clin Invest 2019;129:1030–46.
4. Baba Y, Nosho K, Shima K, Irahara N, Chan AT, Meyerhardt JA, et al. HIF1A overexpression is associated with poor prognosis in a cohort of 731 colorectal cancers. Am J Pathol 2010;176:2292–301.
5. Wang X, Yu M, Zhao K, He M, Ge W, Sun Y, et al. Upregulation of MiR-205 under hypoxia promotes epithelial-mesenchymal transition by targeting ASPP2. Cell Death Dis 2016;7:e2517.
6. Li W, Zong S, Shi Q, Li H, Xu J, Hou F. Hypoxia-induced vasculogenic mimicry formation in human colorectal cancer cells: involvement of HIF-1a, Claudin-4, and E-cadherin and Vimentin. Sci Rep 2016;6:37534.
7. Groulx I, Lee S. Oxygen-dependent ubiquitination and degradation of hypoxia-inducible factor requires nuclear-cytoplasmic trafficking of the von Hippel-Lindau tumor suppressor protein. Mol Cell Biol 2002;22:5319–36.
8. Shan T, Ma J, Ma Q, Guo K, Guo J, Li X, et al. beta2-AR-HIF-1alpha: a novel regulatory axis for stress-induced pancreatic tumor growth and angiogenesis. Curr Mol Med 2013;13:1023–34.
9. Harrell CS, Rowson SA, Neigh GN. Pharmacological stimulation of hypoxia inducible factor-1alpha facilitates the corticosterone response to a mild acute stressor. Neurosci Lett 2015;600:75–9.
10. Ma J, Xue M, Zhang S, Cheng L, Qian W, Duan W, et al. Resveratrol inhibits the growth of tumor cells under chronic stress via the ADRB2HIF1alpha axis. Oncol Rep 2019;41:1051–8.
11. Huang Z, Li G, Zhang Z, Gu R, Wang W, Lai X, et al. beta2AR-HIF-1alpha-CXCL12 signaling of osteoblasts activated by isoproterenol promotes migration and invasion of prostate cancer cells. BMC Cancer 2019;19:1142.
12. Bakadlag R, Jandaghi P, Hoheisel JD, Riazalhosseini Y. The potential of dopamine receptor D2 (DRD2) as a therapeutic target for tackling pancreatic cancer. Expert Opin Ther Targets 2019;23:365–7.
13. Jandaghi P, Najafabadi HS, Bauer AS, Papadakis AI, Fassan M, Hall A, et al. Expression of DRD2 is increased in human pancreatic ductal adenocarcinoma and inhibitors slow tumor growth in mice. Gastroenterology 2016;151:1218–31.
14. Wang X, Wang ZB, Luo C, Mao XY, Li X, Yin JY, et al. The prospective value of dopamine receptors on bio-behavior of tumor. J Cancer 2019;10:1622–32.
15. Lawford BR, Young R, Noble EP, Kann B, Ritchie T. The D2 dopamine receptor (DRD2) gene is associated with co-morbid depression, anxiety and social dysfunction in untreated veterans with post-traumatic stress disorder. Eur Psychiatry 2006;21:180–5.
16. Boehm K, Cramer H, Staroszynski T, Ostermann T. Arts therapies for anxiety, depression, and quality of life in breast cancer patients: a systematic review and meta-analysis. Evid Based Complement Alternat Med 2014;2014:103297.
17. Oliveira Miranda D, Soares de Lima TA, Ribeiro Azevedo L, Feres O, Ribeiro da Rocha JJ, Pereira-da-Silva G. Proinflammatory cytokines correlate with depression and anxiety in colorectal cancer patients. Biomed Res Int 2014;2014:739650.
18. Asahara M, Mushiake S, Shimada S, Fukui H, Kinoshita Y, Kawanami C, et al. Reg gene expression is increased in rat gastric enterochromaffin-like cells following water immersion stress. Gastroenterology 1996;111:45–55.
19. Tanahashi N, Takagi K, Amagasu N, Wang G, Mizuno K, Kawanoguchi J, et al. Effect of acupuncture stimulation on rats with depression induced by water-immersion stress. Neurosci Lett 2016;618:99–103.
20. Kotlyar M, Pastrello C, Pivetta F, Lo Sardo A, Cumbaa C, Li H, et al. In silico prediction of physical protein interactions and characterization of interactome orphans. Nat Methods 2015;12:79–84.
21. Thaker PH, Han LY, Kamat AA, Arevalo JM, Takahashi R, Lu C, et al. Chronic stress promotes tumor growth and angiogenesis in a mouse model of ovarian carcinoma. Nat Med 2006;12:939–44.
22. Gao G, Sun J, Gao J, Xiong L, Yu L, Gao Y. Chronic stress promoted the growth of ovarian carcinoma via increasing serum levels of norepinephrine and interleukin-10 and altering nm23 and NDRG1 expression in tumor tissues in nude mice. Biosci Trends 2013;7:56–63.
23. Frick LR, Arcos ML, Rapanelli M, Zappia MP, Brocco M, Mongini C, et al. Chronic restraint stress impairs T-cell immunity and promotes tumor progression in mice. Stress 2009;12:134–43.
24. Verza FA, Valente VB, Oliveira LK, Kayahara GM, Crivelini MM, Furuse C, et al. Social isolation stress facilitates chemically induced oral carcinogenesis. PLoS One 2021;16:e0245190.
25. Arranz A, Venihaki M, Mol B, Androulidaki A, Dermitzaki E, Rassouli O, et al. The impact of stress on tumor growth: peripheral CRF mediates tumor-promoting effects of stress. Mol Cancer 2010;9:261.
26. Jang HJ, Boo HJ, Lee HJ, Min HY, Lee HY. Chronic stress facilitates lung tumorigenesis by promoting exocytosis of IGF2 in lung epithelial cells. Cancer Res 2016;76:6607–19.
27. Fatakia SN, Costanzi S, Chow CC. Molecular evolution of the transmembrane domains of G protein-coupled receptors. PLoS One 2011;6:e27813.
28. Purgert CA, Izumi Y, Jong YJ, Kumar V, Zorumski CF, O'Malley KL. Intracellular mGluR5 can mediate synaptic plasticity in the hippocampus. J Neurosci 2014;34:4589–98.
29. Wright CD, Wu SC, Dahl EF, Sazama AJ, O'Connell TD. Nuclear localization drives alpha1-adrenergic receptor oligomerization and signaling in cardiac myocytes. Cell Signal 2012;24:794–802.
30. Joyal JS, Nim S, Zhu T, Sitaras N, Rivera JC, Shao Z, et al. Subcellular localization of coagulation factor II receptor-like 1 in neurons governs angiogenesis. Nat Med 2014;20:1165–73.
31. Xiao T, Zhang Q, Zong S, Zhong WL, Qin Y, Bi Z, et al. Protease-activated receptor-1 (PAR1) promotes epithelial-endothelial transition through Twist1 in hepatocellular carcinoma. J Exp Clin Cancer Res 2018;37:185.
32. Brahimi-Horn MC, Chiche J, Pouyssegur J. Hypoxia and cancer. J Mol Med 2007;85:1301–7.
33. Hockel M, Vaupel P. Tumor hypoxia: definitions and current clinical, biologic, and molecular aspects. J Natl Cancer Inst 2001;93:266–76.
34. Rofstad EK, Danielsen T. Hypoxia-induced metastasis of human melanoma cells: involvement of vascular endothelial growth factor-mediated angiogenesis. Br J Cancer 1999;80:1697–707.
35. Kamura T, Sato S, Iwai K, Czyzyk-Krzeska M, Conaway RC, Conaway JW. Activation of HIF1alpha ubiquitination by a reconstituted von Hippel-Lindau (VHL) tumor suppressor complex. Proc Natl Acad Sci U S A 2000;97:10430–5.

36. Lewis MD, Roberts BJ. Role of nuclear and cytoplasmic localization in the tumour-suppressor activity of the von Hippel-Lindau protein. Oncogene 2003; 22:3992–7.
37. Sudeshna G, Parimal K. Multiple non-psychiatric effects of phenothiazines: a review. Eur J Pharmacol 2010;648:6–14.
38. Qian K, Sun L, Zhou G, Ge H, Meng Y, Li J, et al. Trifluoperazine as an alternative strategy for the inhibition of tumor growth of colorectal cancer. J Cell Biochem 2019;120:15756–65.
39. Feng Z, Xia Y, Gao T, Xu F, Lei Q, Peng C, et al. The antipsychotic agent trifluoperazine hydrochloride suppresses triple-negative breast cancer tumor growth and brain metastasis by inducing G0/G1 arrest and apoptosis. Cell Death Dis 2018;9:1006.
40. Bhat K, Saki M, Vlashi E, Cheng F, Duhachek-Muggy S, Alli C, et al. The dopamine receptor antagonist trifluoperazine prevents phenotype conversion and improves survival in mouse models of glioblastoma. Proc Natl Acad Sci U S A 2020;117:11085–96.